JCB Article

Small cargo proteins and large aggregates can traverse the Golgi by a common mechanism without leaving the lumen of cisternae

Alexander A. Mironov,[1] Galina V. Beznoussenko,[1] Paolo Nicoziani,[1] Oliviano Martella,[1] Alvar Trucco,[1] Hee-Seok Kweon,[1] Daniele Di Giandomenico,[1] Roman S. Polishchuk,[1] Aurora Fusella,[1] Pietro Lupetti,[2] Eric G. Berger,[3] Willie J.C. Geerts,[4] Abraham J. Koster,[4] Koert N.J. Burger,[4] and Alberto Luini[1]

[1]Department of Cell Biology and Oncology, Istituto di Ricerche Farmacologiche "Mario Negri," 66030 Santa Maria Imbaro, Chieti, Italy
[2]Dipartimento di Biologia Evolutiva, Università di Siena, 453100 Siena, Italy
[3]Institute of Physiology, University of Zurich, CH-8057 Zurich, Switzerland
[4]Department of Molecular Cell Biology, Institute of Biomembranes, Utrecht University, 83584 CH Utrecht, Netherlands

Procollagen (PC)-I aggregates transit through the Golgi complex without leaving the lumen of Golgi cisternae. Based on this evidence, we have proposed that PC-I is transported across the Golgi stacks by the cisternal maturation process. However, most secretory cargoes are small, freely diffusing proteins, thus raising the issue whether they move by a transport mechanism different than that used by PC-I. To address this question we have developed procedures to compare the transport of a small protein, the G protein of the vesicular stomatitis virus (VSVG), with that of the much larger PC-I aggregates in the same cell. Transport was followed using a combination of video and EM, providing high resolution in time and space. Our results reveal that PC-I aggregates and VSVG move synchronously through the Golgi at indistinguishable rapid rates. Additionally, not only PC-I aggregates (as confirmed by ultrarapid cryofixation), but also VSVG, can traverse the stack without leaving the cisternal lumen and without entering Golgi vesicles in functionally relevant amounts. Our findings indicate that a common mechanism independent of anterograde dissociative carriers is responsible for the traffic of small and large secretory cargo across the Golgi stack.

Introduction

Understanding the organization of the biosynthetic pathway has been a goal of cell biology for the last few decades (Mellman and Warren, 2000). However, despite persistent efforts, the principles of operation of this pathway remain unclear. Current research in this area focuses on three different models. One, the vesicular traffic model, envisions that secretory compartments are stable entities and that proteins are transported from each compartment to the next inside small round vesicles. This scheme has dominated the field for the last few decades, and has provided an elegant framework by which to rationalize a wealth of molecular and genetic data (Rothman and Wieland, 1996; Schekman and Orci, 1996); however, it has never been validated in vivo, and in recent years it has come under increasing criticism. The second is the progression–maturation scheme, by which cargo remains confined within the lumen of cisternae while cisternae move through the stack by gradually maturing from cis into trans compartments (Bannykh and Balch, 1997; Mironov et al., 1997; Glick and Malhotra, 1998). The third model (flow through continuities) posits that cargo flows along permanent or transient continuities, connecting successive compartments (Weidman, 1995; Mironov et al., 1997, 1998).

To resolve these uncertainties, we have developed experimental models to study the traffic of large secretory aggregates (Bonfanti et al., 1998), and a technique integrating dynamic

The online version of this article contains supplemental material.

Address correspondence to A. Luini, Department of Cell Biology and Oncology, Consorzio Mario Negri Sud, Via Nazionale, 66030 Santa Maria Imbaro, Chieti, Italy. Tel.: 39-0872-570-323. Fax: 39-0872-570-412. E-mail: luini@dcbo.cmns.mnegri.it

A. Mironov and G.V. Beznoussenko contributed equally to this work.

*Abbreviations used in this paper: AA, ascorbic acid; CGN, cis-Golgi network; COP, coat protein; DPD, 2,2-dipyridyl; FKBP, FK506-binding protein; GFP, green fluorescent protein; GM, Golgi matrix protein; GT, galactosyltransferase, IC, intermediate compartment; NEM, *N*-ethylmaleimide; PC, procollagen; TGN, trans-Golgi network; VSVG, vesicular stomatitis virus G protein.

Key words: intracellular traffic; Golgi complex; transport vesicles; procollagen; VSVG

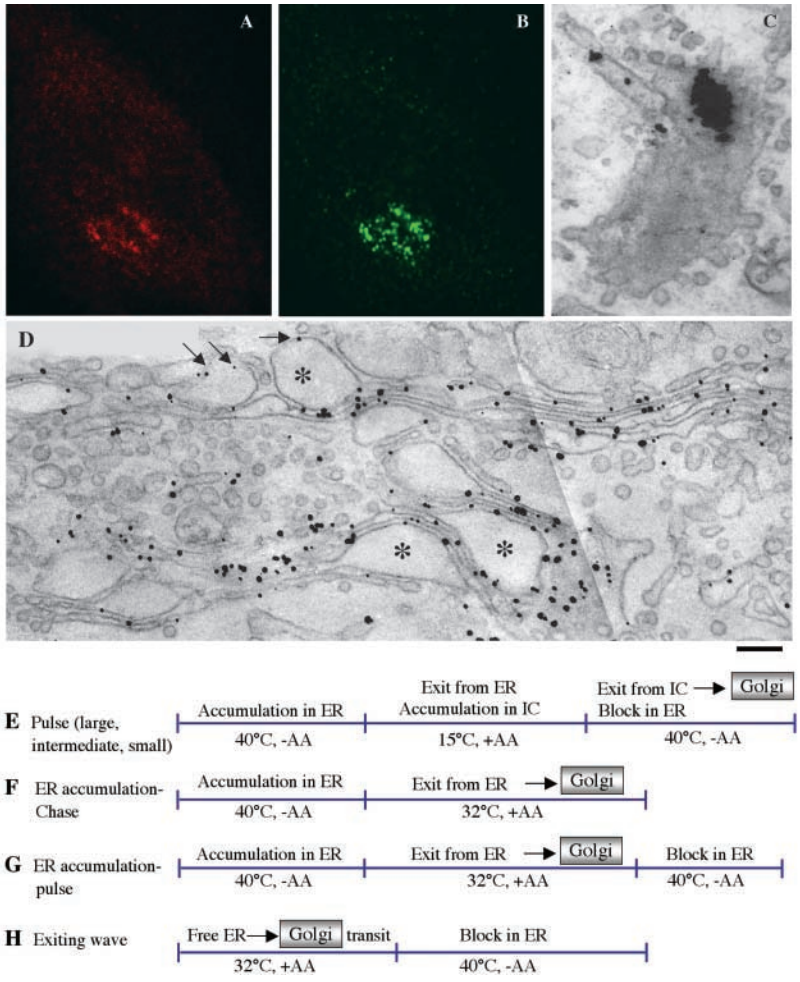

Figure 1. **Human fibroblasts can express and transport both PC-I aggregates and VSVG through the Golgi complex.** Human fibroblasts were stimulated to synthesize PC-I and infected with ts045-VSV. After accumulation of both and PC-I and VSVG in the ER at 40°C for 3 h, cells were shifted to 32°C for 9 min and then fixed, permeabilized with saponin, and prepared for immunofluorescence or fixed and prepared for immuno-EM. (A and B) Immunofluorescent double labeling for VSVG (red) and PC-I (green). Both cargoes localize mostly in the Golgi area. The two labeling patterns are very similar. (C) Immuno-EM labeling of PC-I by the preembedding nanogold gold enhancement technique. An aggregate appears as thick cluster of gold particles in a tangential section of a Golgi cisterna. (D) Immuno-EM labeling of VSVG by the same technique. VSVG is distributed throughout the Golgi membranes, including PC-I–containing distensions. Many typical cisternal distensions (*) are seen within the Golgi ribbon (arrows). (E–H) Synchronization protocols. (E) Pulse protocols: cells were kept at 32°C in the presence of AA (50 μg/ml) for 3 h, shifted to 40°C for 3 h (in some experiments 1–2 h), and then shifted to 15°C for 2 h (large pulse), 45 min (intermediate pulse), or 15 min (small pulse), and finally shifted back to 40°C. (F) ER accumulation–chase: cells were kept at 40°C for 3 h in the absence of AA, and then shifted to 32°C in the presence of AA. (G) ER accumulation–pulse: same as for ER accumulation–chase except that cells were shifted back to 40°C after 5 min at 32°C. (H) Exiting wave protocol (Results). Bar: (A and B) 200 nm; (C and D) 2 μm.

green fluorescent protein (GFP)*-based light microscopy and EM (correlative video light EM) (Mironov et al., 2000; Polishchuk et al., 2000). Using these approaches, we have previously established that large procollagen (PC)-I aggregates (300–400 nm in length compared with secretory vesicles 65 nm in diameter) traverse the Golgi stack without leaving the lumen of Golgi cisternae. We have also proposed cisternal progression maturation as the most likely mechanism of transport, although other traffic schemes have not been excluded (Bonfanti et al., 1998; Griffiths, 2000). However, large secretory aggregates are relatively rare and may be restricted to special cells. Most other cargoes are small freely diffusing molecules that could use alternative modes of transport. For instance, it has been hypothesized by us and others (Mironov et al., 1998; Pelham and Rothman, 2000) that, whereas large nondiffusable objects such as PC-I aggregates might be transported by the cisternal maturation mechanism, small molecules able to diffuse freely might move faster through the Golgi via coat protein (COP)I vesicles (Pelham and Rothman, 2000; Volchuk et al., 2000) or transport tubules (Weidman, 1995; Mironov et al., 1997, 1998).

The aim of this study is to determine whether the transport mechanism used by PC-I applies only to supramolecular aggregates, or is a universal mechanism for the majority of the secretory molecules. To address this question, we have developed a set of synchronization protocols and a suitable model system to compare the transport of PC-I and the vesicular stomatitis virus G protein (VSVG), a well-characterized diffusable membrane protein traffic marker (Bergmann, 1989), in the same cell. Specifically, we have examined two interrelated questions: (a) Are VSVG and PC-I transported at the same or different rates through the Golgi (if they are transported by different mechanisms they should move at different rates)?; and (b) Does VSVG, like PC-I, move through the Golgi without leaving the lumen of cisternae, and hence without a requirement for vesicular carriers? Our collective observations compel us to propose that a single rapid transport mechanism not requiring physical transfer of cargo from Golgi cisterna to cisterna via dissociative carriers accounts for the movement of both PC-I and VSVG through the Golgi complex.

Results

Development of an assay to monitor VSVG and PC-I transport in the same cell

The rate of secretory traffic varies depending on cell type and experimental conditions. Therefore, to compare the transport of VSVG and PC-I, it was necessary to develop (a) a cellular system expressing both cargoes; and (b) a repertoire of conditions allowing us to synchronize the transport of the two cargoes and control their amount and timing of arrival to the Golgi.

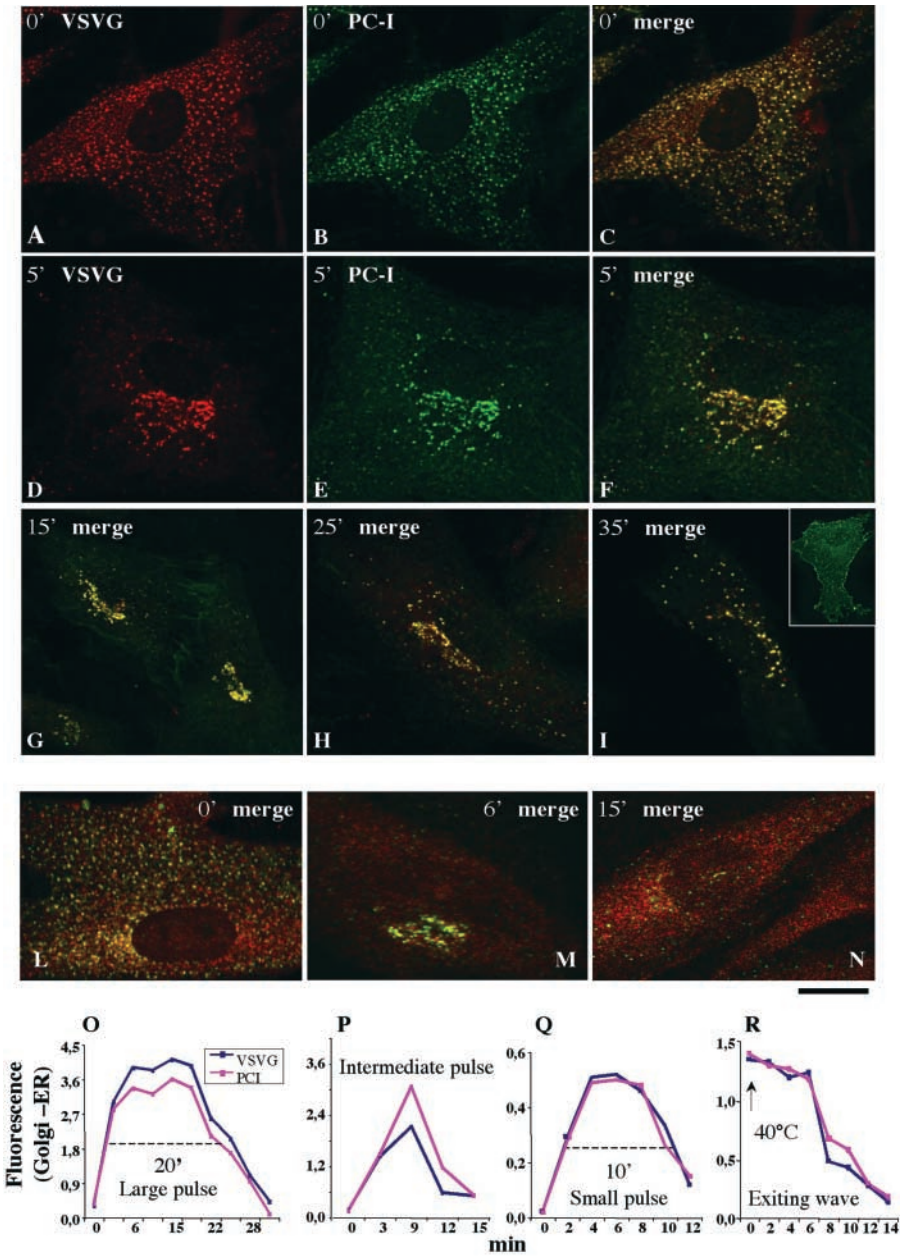

Figure 2. **PC-I and VSVG are transported through the Golgi complex at indistinguishable rates.** Human fibroblasts were subjected to different synchronization protocols (see below), fixed at the times indicated in the figure after release of the temperature block, and then double immunolabeled for PC-I and VSVG. For the sake of space, in most panels the two colors are presented only in the merged form. (A–I) Large-pulse protocol. (L–N) Small-pulse protocol. The inset in panel I shows labeling for VSVG on the membrane surface (labeled without permeabilization with an antibody against the lumenal epitope). The colocalization between PC-I and VSVG was significant at all time points. (O–R) Quantification and time course of the passage of VSVG and through the Golgi under the large-, small-, and intermediate-pulse, and exiting-wave protocols. The values were obtained by measuring the average fluorescence intensities (in arbitrary units) of each cargo in the Golgi area and in the nuclear envelope (ER, with average fluorescence of 1). The differences between the Golgi and the ER values for each cargo were then calculated and plotted as a function of time. Clearly, this difference (Golgi minus ER) increases as cargoes exit the ER and enter the Golgi, and then it decreases when the cargoes exit the Golgi for the plasma membrane. The average transit time of the cargoes through the Golgi area is defined as the lag (indicated by the discontinuous line in O and Q) between the half time of the rising phase and that of the decay phase. The transit time was ~20 min for the large-pulse, and 8–10 min for the small- and intermediate-pulse protocols. The cargo clearance time from the Golgi under the exiting-wave protocol is defined as the lag between the start of the 40°C block and the half time of the decay phase of the curve (R); it was ~7–8 min. It is apparent that VSVG and PC-I move simultaneously through the Golgi area under all the protocols, whereas the rate of traffic differs between protocols. Each value represents the average of 7–15 independent measurements from at least three different experiments. The SDs did not exceed 15% of the mean. Bar, 10 μm.

Human fibroblasts are flat and suitable for morphological transport assays. When kept in growth medium (10% FCS) they synthesize PC-I in low amounts, but can be switched into a more differentiated PC-I–producing state by replacing 10% fetal calf serum with 1% adult calf serum for 3–10 h. Under the latter conditions, their rate of PC-I secretion is comparable to that of other "professional" PC-I secretors (Bonfanti et al., 1998). When infected with VSV at low concentrations for short incubation times (see Materials and methods), they express measurable amounts of the VSVG without significantly losing expression of PC-I (Fig. 1, A–D). They can also be transfected with VSVG or VSVG–GFP by electroporation. Thus, they are suitable for studies of dual PC-I and VSVG cargo transport.

Synchronization of PC-I and VSVG transport was achieved by controlling the exit of both cargoes from the ER and the intermediate compartment (IC). To inhibit the exit of VSVG from the ER, we used the temperature-sensitive variant of VSVG (tsVSVG, produced by the ts045-VSV viral strain), which does not fold and accumulates in the ER at 40°C. Because tsVSVG was used in all experiments involving VSVG (see Materials and methods), it will henceforth be referred to simply as VSVG. The block of VSVG in the ER can be reverted by shifting the temperature to 32°C or lower (Bergmann, 1989). To prevent the exit of PC-I from the ER, one can deprive the medium of ascorbic acid (AA), as AA is an essential cofactor of prolyl-hydroxylase and PC-I does not fold if its prolines are insufficiently hydroxylated (Harwood et al., 1976), and/or add the inhibitor of prolyl-

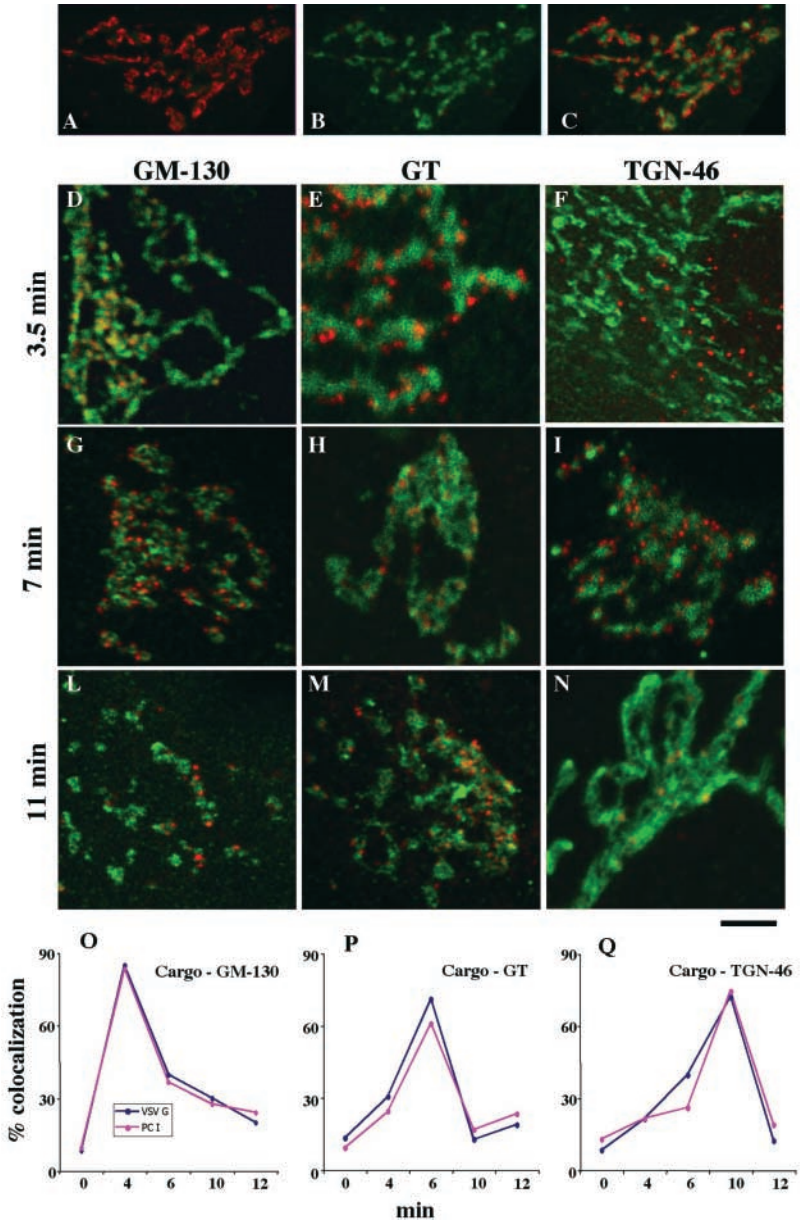

Figure 3. **PC-I and VSVG move through the main Golgi subcompartments (cis-, medial-, and trans-TGN) at indistinguishable rates.** Human fibroblasts were fixed at steady state (A–C) or subjected to the small-pulse protocol and fixed at various times after release of the 15°C block (D–N). (A–C) Golgi areas stained for GM130 (A, red) and TGN (B, green); the merged image is shown in C. Note that the patterns of two colors appear very similar in (A) and (B), but they clearly do not overlap (C). (D–N) Cells subjected to the small-pulse protocol were fixed at the times indicated in the figure after releasing the 15°C block and double labeled for VSVG and GM130 (D, G, and L), VSVG and GT (E, H, and M), or VSVG and TGN (F, I, and N). VSVG is red and GM130, GT, and TGN are green. At time 0, VSVG localized in peripheral spots (IC elements) and did not overlap with the Golgi markers (unpublished data). At 3.5 min, VSVG colocalized with GM130 (D) but not with GT (E) and TGN46 (F). Later (7 min), VSVG lost colocalization with GM130 (G) acquired colocalization with GT (H), and did not colocalize with TGN46 (I). Finally (11 min), VSVG lost colocalization with GM130 (L) and GT (M) and acquired colocalization with TGN46 (N). Identical results were obtained by labeling PC-I instead of VSVG (see below), and the two cargoes colocalized perfectly (unpublished data). (O–Q) Quantification and time course of the passage of VSVG and PC-I through the main Golgi subcompartments. The localization of cargoes in each subcompartment was assessed by measuring the degree of overlap of each cargo with the marker of each subcompartment (GM130, GT, and TGN) (see Materials and methods), and is expressed as the percentage of colocalization (percentage of cargo-containing pixels which also contain the appropriate Golgi marker). It is apparent that the two cargoes move together. Each value represents the average of eight to fourteen independent measurements from at least three different experiments. The SDs did not exceed 15% of the mean. Bar: (A–C) 12 μm; (D, F–I, L, and M) 10 μm; (E and H) μm 7,5; (N) 5 μm.

hydroxylation 2,2-dipyridyl (DPD) (Bonfanti et al., 1998). Additionally, the PC-I folding block can be enhanced by high temperatures (e.g., 40°C) (Bruckner and Eikenberry, 1984). The PC-I retention in the ER can be rapidly reversed by adding AA to the medium and downshifting the temperature. The traffic of both VSVG and PC-I can also be stopped by immobilizing the IC near the ER at 15°C (Kuismanen and Saraste, 1989), and this block can be released by upshifting the temperature.

By combining these two traffic blocks and varying their sequence and duration, a number of synchronization protocols can be developed to manipulate the amount and timing of the arrival of cargo in the Golgi ribbon; there are three main protocols (scheme in Fig. 1). One type was designed to generate a short "pulse" of secretory material impinging on the Golgi complex. This was achieved by accumulating PC-I and VSVG in the ER at 40°C without AA, letting them pass in the IC (at 15°C with AA), and then shifting the temperature back to 40°C (and removing AA) to release the exit block from the IC and, at the same time, reinstate the exit block from the ER. For brevity, as AA is always absent during the 40°C block and present at lower temperatures, AA will henceforth not be specifically mentioned. Note that once PC-I and VSVG have moved out of the ER, they maintain their folding and are transported normally at 40°C (Bruckner and Eikenberry, 1984; Lyles and McKenzie, 1998). In contrast, if they are still in the ER, they can rapidly unfold upon shifting the temperature back to 40°C, and can be retained in this organelle (Bruckner and Eikenberry, 1984; Lyles and McKenzie, 1998); this results in a very rapid exit block from the ER. A useful feature of the pulse scheme is that the size of the pulse (amount of cargo) can be controlled by varying the length of the blocks. For instance, by accumulating a large amount of cargo in the ER and then trapping most of it in the IC with a long 15°C block, one creates a large pool of cargo ready to be released from the IC

into the Golgi. In contrast, 15°C blocks of a shorter or intermediate length provide smaller pools of cargo in the IC ready to move onward. This is important because the size of the pulse affects the traffic behavior of the Golgi (see below). We call these protocols large-, intermediate-, and small-pulse schemes, respectively. A second protocol was designed to accumulate unfolded cargo in the ER at 40°C, and then let it fold and exit from this organelle synchronously at 32°C; it has been widely used in the literature. We call this ER accumulation–chase protocol. A pulsed variation of this is obtained by reinstating the ER exit block after a short period of release at 32°C (ER accumulation–pulse). A third protocol was designed to let traffic reach a steady state at 32°C, suddenly block the exit of cargo from the ER by shifting the temperature to 40°C, and monitor the exit of cargo from the Golgi; we call this exiting-wave protocol. Using these schemes (Fig. 1), we have addressed three interrelated issues: (a) Do PC-I and VSVG move at the same or different rates through the Golgi?; (b) Do PC-I and VSVG physically pass from one cisterna to the next cisterna or remain always in the same cisterna while transiting through the stack?; and (3) Do PC-I and VSVG enter dissociative vesicular carriers to traverse the Golgi complex?

PC-I and VSVG traverse the Golgi complex at fast indistinguishable rates under different experimental conditions

First, we used the large-pulse protocol, which results in a large buildup of PC-I and VSVG in the IC. Fig. 2 shows by immunofluorescence that when the cells were shifted from 40 to 15°C, both cargoes exited the ER and, after 2 h, were present in numerous bright spots (IC elements) distributed throughout the cytoplasm. PC-I and VSVG exhibited a good degree of overlap in these structures. When the temperature was shifted back to 40°C, the distribution of both proteins in the IC began to change 3–4 min later: PC-I and VSVG came closer to the Golgi, and at 4–5 min they had reached the Golgi area (identified by the bona fide Golgi marker giantin, unpublished data) where they resided for an average of 20 min (transit time, legend to Fig. 2). Finally, both cargoes exited the Golgi together in distinct spots, probably representing post-Golgi carriers, in which they colocalized. (Fig. 2, A–I). Thus, the rates of passage of PC-I and VSVG through the secretory system were indistinguishable.

The amount of cargo reaching the Golgi per unit time in this experiment is probably much larger than during physiological traffic. To examine the behavior of the transport pathway under conditions closer to normal, we used the small-pulse protocol in which the accumulation of cargo in the IC is reduced but still sufficient to allow the formation of visible cargo-containing IC elements (scheme in Fig. 1). In spite of some fluorescence background due to cargo remaining in the ER, it was clear that, after release of the 15°C block, PC-I and VSVG colocalized and reached the Golgi simultaneously within 3–4 min, resided in the Golgi area for ~8 min (transit time, legend to Fig. 2), and then left it, again simultaneously (Fig. 2, L–N). Thus, the movements of PC-I and VSVG could not be dissociated, even using this protocol. Notably, the cargoes in the Golgi area were discontinuously distributed in 10–30 discrete fluorescent spots of variable intensities (Fig. 3 and see Fig. 8). Also, interestingly, the transit time of the two cargoes through the Golgi area was shorter than when using the large-pulse protocol (8 vs. 20 min; quantification in Fig. 2, O and Q), suggesting that the transport behavior of the Golgi is influenced by the amount of cargo processed per unit time. This cargo effect is being analyzed separately.

The other three protocols (ER accumulation–chase, exiting-wave, and intermediate-pulse) were used to compare the traffic rates of VSVG and PC-I. Again, the behavior of the two cargoes could not be distinguished (quantification in Fig. 2, O–R). Of note is that the clearance time of both cargoes in the exiting-wave protocol was ~8 min or less (Fig. 2 R), similar to the residence time seen using the small-pulse protocol. Because under the exiting-wave scheme transport proceeds at steady state until exit from the ER is blocked, and the Golgi does not experience the potentially perturbing pulse of cargo to which it is subjected in other protocols, 8 min should represent the through-Golgi transit time at steady state at 40°C.

To compare the traffic of PC-I and VSVG in a quantitative fashion, the fractions of the cargoes present in the Golgi area at each time point were measured (legend to Fig. 2) and plotted. Fig. 2, O–R, visually renders the strikingly parallelism of the traffic of PC-I and VSVG through the Golgi under all the synchronization protocols.

Because the Golgi area contains diverse structures, we next analyzed the progression of the two cargoes through the main Golgi subcompartments, namely the cis-Golgi network (CGN), the stack, and the trans-Golgi network (TGN), by relating the localization of PC-I and VSVG to the known markers of these compartments, the Golgi matrix protein (GM)130, galactosyl-transferase (GT), and TGN46. This is possible by immunofluorescence microscopy in these cells, as can be seen in Fig. 3, A–C, most likely because the noncisternal components of the CGN and TGN extend sufficiently far from the side of the stack (as can be appreciated by inspecting their ultrastructure; unpublished data) to allow for partial resolution of these three compartments at the light microscopy level. The small-pulse protocol was again used for these experiments. Both cargoes reached the Golgi area 3–4 min after release of the block. At this time, their colocalization with GM130 was good, with GT poor, and with TGN-46 nearly absent, indicating that they resided in the CGN. During the next 2–3 min, the overlap of the cargoes with GM130 decreased and that with GT increased, indicating that cargo transfer into the stacks was taking place. PC-I and VSVG then remained in the GT zone until ~10 min, and finally shifted toward the TGN (judging from colocalization with TGN-46) where they remained until released from the Golgi in post-TGN carriers (Fig. 3, D–N). Thus, three stages of traffic in the Golgi area can be distinguished, throughout which PC-I and VSVG colocalize nearly perfectly (see below) and transit together at the same rates. The degree of overlap of each of the two cargoes with the markers of the three Golgi subcompartments during passage through the Golgi can be quantified. The results (Fig. 3, O–Q) underscore once again the remarkable coupling between the movements of the two cargoes, and confirm with

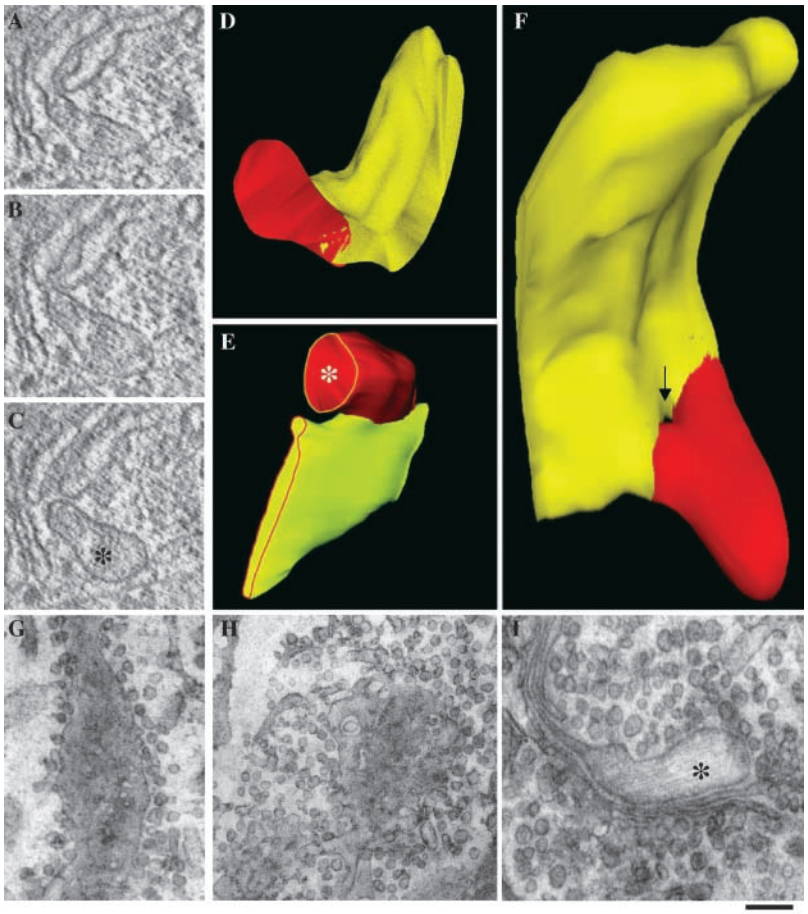

Figure 4. **PC-I-containing distensions never dissociate from Golgi cisternae during intra-Golgi traffic.** Human fibroblasts were subjected to the large ER accumulation–chase protocol (or to the large-pulse protocol) and fast frozen (A–F) or treated with NEM to inhibit vesicle fusion (G–I). (A–F) 9 min after the shift to 32°C, the cells were fixed by ultra-fast freezing, and then cryosubstituted and embedded into Epon 812. Thick (250 nm) sections of Golgi cisternae were cut, prepared for electron microscopic tomography, and virtual 2–3-nm slices (A–C) were extracted from the tomograms using the IMOD software (Ladinsky et al., 1999). The 3-D reconstruction and surface rendering of the cisternae (yellow) and distensions (red) were performed using the SURFdriver program. The same structure is shown in two orientations (D and F). The image in F was chosen to show a pore in the cisterna which generates the impression of discontinuity between distension and cisterna in one of the virtual sections (arrow). Serial thin (50 nm) sections of Golgi cisternae were cut and used to reconstruct the image in E. (G–I) NEM treatment. 7 min after releasing the temperature block, cells were placed on ice, and medium with (H and I) or without (G) NEM (100 μM) was added for 15 min. After washing on ice, cells were shifted to 40°C again for an additional 3 min, and then fixed and prepared for EM. Tangential section of a cisterna with surrounding vesicles in a control cell (G). Tangential section of a cisterna in a NEM-treated cell; vesicular profiles are much more numerous (three- to fourfold) than in controls (H). PC-I distension connected with a cisternae in a NEM-treated cell (I). *, PC-I–containing distensions. Bar: (A and C–E) 150 nm; (F) 100 nm; (G and H) 300 nm; (I) 200 nm.

a high degree of precision that VSVG and PC-I move together through the transport pathway. Similar results were obtained, with higher spatial resolution, in immuno-EM experiments (see Figs. 5 and 6 and related text).

Notably, in the experiments in Figs. 2, L–N, and 3, the cargoes were not homogeneously distributed through the Golgi ribbon, rather, they were restricted to 10–30 discrete fluorescent spots (always containing both PC-I and VSVG; unpublished data) of variable intensity and apparent size between 1 and 2 microns scattered throughout the ribbon, whereas a large fraction of the Golgi area was empty of cargo. The significance of these unexpected observations is discussed further below (see Figs. 5 and 8, related text, and Discussion).

Finally, we examined whether PC-I and VSVG might be physically linked in some way (e.g., via a lumenal matrix) or might somehow mutually influence each other's movements in these cells. To this end, the traffic rates of the two cargoes were studied in human fibroblasts expressing either only PC-I or only VSVG (the latter condition was obtained by shutting down PC-I synthesis by keeping the cells in 10% FCS). The progression of each of the two cargoes through the Golgi occurred at rates very similar to those seen when they were expressed together (i.e., with an average intra-Golgi transit times of 8–10 min for both) (unpublished data). Also, when the same experiment was repeated looking at VSVG in COS-7 cells, the same intra-Golgi transit time was observed (unpublished data).

PC-I aggregates traverse the Golgi without leaving the cisternae in megavesicles

PC-I has been reported to move along the secretory system without dissociating from cisternae (Bonfanti et al., 1998). However, because another type of secretory aggregates has been seen in containers (called megavesicles, 300–400 nm in diameter) adjacent to, but physically separate from, Golgi cisternae (Volchuk et al., 2000), we decided to reverify our previous proposition using new approaches. In our previous experiments, we had used standard fixation techniques for EM. Chemical fixation, albeit validated in countless experiments, is always a potential source of artifacts. For instance, in theory, if PC-I–containing megavesicles exist, they might be made to fuse with neighboring cisternae by the fixatives. This would mask evidence for their existence. To overcome this problem, we used ultrafast cryofixation, a virtually artifact-free method (Erk et al., 1998), and a synchronization protocol ensuring a high flux of PC-I, and therefore a large number of PC-I aggregates moving through the Golgi stacks. Both the ER accumulation–chase and the large-pulse protocols were used. Under both conditions, 6–8 min after release of the temperature block, all of the stacks exhibited numerous PC-I aggregate–containing distensions. Cryofixed cells were serial sectioned to establish the 3-D structure of these aggregates. Out of 120 distensions observed, none was found to be disconnected from the Golgi cisternae, either in thick sections (250 nm) subjected to electron tomography

(Koster et al., 1997; Ladinsky et al., 1999) or in traditional thin sections. Fig. 4, D–F shows representative 3-D reconstructions of PC-I–containing distensions illustrating the above conclusion.

Another potential reason for failing to observe the hypothetical PC-I megavesicles is that these structures might be too transient to be seen with our previous experimental set up. Given the high number of PC-I aggregates sectioned to date in this and previous work (Bonfanti et al., 1998), this seems very unlikely. Regardless, we reasoned that if PC-I megavesicles normally form but fuse immediately with the acceptor cisterna, they should accumulate, and hence become detectable, if fusion is inhibited. The protein NSF is essential in the known pathways of Golgi membrane fusion (including fusion of COPI vesicles to Golgi cisternae), and can be relatively selectively inactivated by the reagent *N*-ethylmaleimide (NEM) under controlled conditions (Malhotra et al., 1988). Cells were treated with NEM just after PC-I had reached the Golgi stack, and fixed 3–5 min later. To verify the efficacy of this treatment, we counted the number of COPI-dependent vesicles after exposure to NEM (because NEM does not block vesicle formation, vesicles should accumulate in cells treated with this drug) (Malhotra et al., 1988). As expected, round profiles with the appearance expected for COPI vesicles increased in number to levels threefold higher than basal values, confirming that NEM had inhibited vesicle fusion. Yet, when PC-I–containing distensions were examined, they were again found to be always connected to cisternae, further indicating that these structures never dissociate, even transiently (Fig. 4, G–I).

As shown above, PC-I traverses the Golgi relatively rapidly, with an average of time of 8–10 min. This is seemingly dissimilar from previous measurements in chick embryo fibroblasts (Bonfanti et al., 1998), indicating that although 50–60% of the PC-I aggregates exit the cis-Golgi in 10 min, a significant fraction of PC-I remains in the Golgi for >1 h. This might suggest the existence of two phases in the efflux of PC-I from the Golgi, one fast and one slow. Based on this data, Volchuk et al. (2000) have hypothesized that the traffic of PC-I is a relatively slow process. However, upon reinvestigating our previous experimental conditions, we found that the slow second phase was only apparent, and, in fact, simply reflected the fact that, under the conditions used in those experiments, PC-I aggregates, after a first rapid decrease, reached a plateau which lasted for several hours and was relatively high (25–30% of the basal levels; unpublished data). This plateau might have generated the impression of a very slow PC-I clearance from the Golgi. However, it was instead due to the fact that the hydroxylation/folding block induced by the PC-I prolyl-hydroxylase inhibitor DPD (Bonfanti et al., 1998) and the consequent exit block from the ER, were partially "leaky." As a result, although PC-I aggregates exited the Golgi at normal speed, they were continuously replaced by PC-I escaping the block. This was confirmed by the finding that in further experiments where the hydroxylation blocker DPD was used at higher concentrations, no such plateau was observed, and PC-I exited the Golgi at a uniformly fast rate (unpublished data). Higher DPD doses had not been used routinely in our previous experiments because they were close to the threshold for toxicity. Our present protocols in human fibroblasts are not affected by this drawback (the folding block is achieved by withdrawal of AA and high temperature, a nontoxic condition) and we observe monophasic rapid PC-I traffic rates. In line with our present measurements, previous studies (Cho and Garant, 1981; Leblond, 1989) based on radiolabeling and autoradiography report an average residence time of PC-I in the Golgi complex in the 10–20-min range.

VSVG molecules traverse the stack without physically passing form cisterna to cisterna and without entering Golgi vesicles

The observation that VSVG and PC-I travel at indistinguishable rates (therefore presumably by the same transport mechanism) suggests that VSVG, like PC-I, does not need enter dissociative vesicular carriers for intra-Golgi traffic. To verify this proposition, we designed a strategy to visually isolate a pool of VSVG located in a single Golgi cisterna, and then examined how this VSVG pool moves onward during intra-Golgi transit. This can be achieved by delivering the smallest possible synchronized load of VSVG to the Golgi complex, again by using the small-pulse protocol. If the pulse is sufficiently short-lasting and small, the VSVG, independently of its mode of entry in the Golgi, should be incorporated in only one cis-Golgi cisterna, at least in some of the stacks. Later, when the pulse is exhausted, incoming IC elements will be devoid of VSVG. If this scheme works, at least two scenarios are possible, and will be considered in this section. One is that VSVG moves continuously from cisterna to cisterna via vesicles (vesicular traffic). This should result in two observations: (a) VSVG should appear to diffuse from the starting cisterna onward, creating a gradient of cargo through the stack; and (b) VSVG should be enriched, or at least not depleted, in the Golgi carrier vesicles (this is the most reasonable prediction under this model; see Discussion). In contrast, in the second scenario (PC-I–like traffic), VSVG should (a) remain in the cisterna in which it had been incorporated in the first place, as the cisterna moves onward; and (b) Golgi vesicles should be depleted of VSVG. A third possibility (flow of cargo via dynamic continuities between heterologous cisterna) will be treated separately (see Discussion).

The first question, Does VSVG remain within a single cisterna or does it equilibrate through the stack by passing from cisterna to cisterna during transit?, was addressed in the experiments in Fig. 5. Panels A–E show the progression of VSVG through the stack by immunogold labeling. These experiments were carried out in both human fibroblasts and COS-7 cells, with similar results. At time 0, the stacks were empty and VSVG was in small clusters of convoluted tubules with the morphology of IC elements (unpublished data). 3 min later, VSVG was in IC elements in the vicinity of the Golgi and in a flattened reticular cisterna at one pole of the stack (Fig. 5 A). Both of these structures labeled for the cis-Golgi marker GM130. Later, between minutes 4 and 9, VSVG moved through the stack (Fig. 3). This is the period during which the distribution of VSVG is expected to differentiate between intra-Golgi traffic mechanisms. At 7 min, the localization pattern of VSVG was striking. In a substantial fraction of the stacks (~30–40%), VSVG was re-

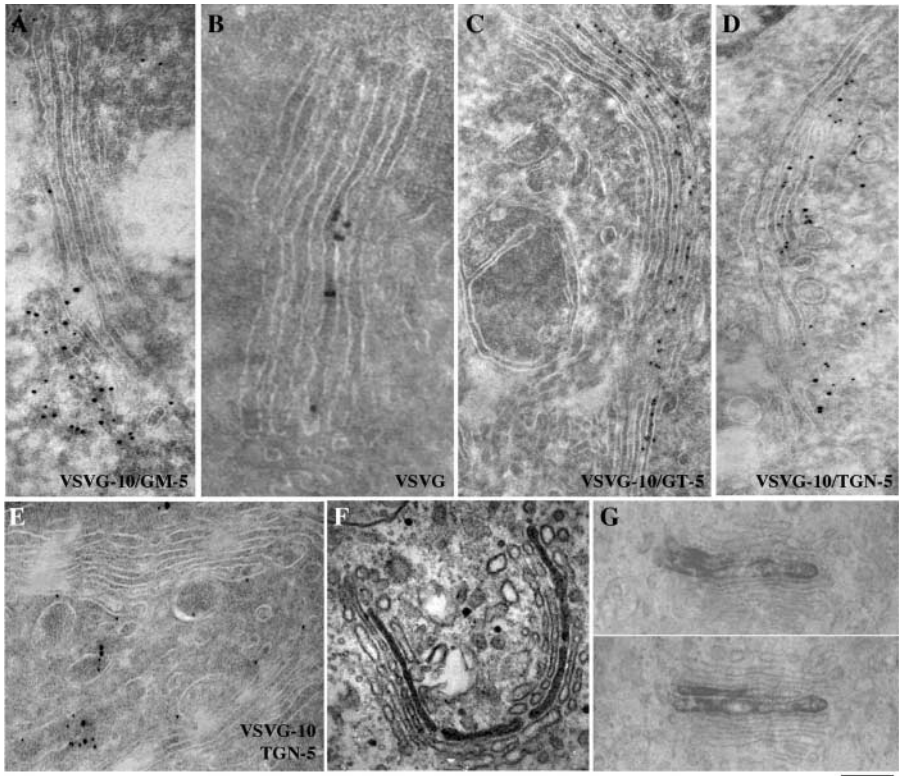

Figure 5. **VSVG transits through the Golgi without equilibrating across the stack, i.e., while remaining in the same cisterna.** Human fibroblasts and COS-7 cells were subjected to the small-pulse protocol, fixed at the times indicated below after release of the 15°C block, and prepared for immunogold labeling for VSVG (10-nm particles), and the Golgi markers GM130, GT, and TGN46 (5- nm particles). Before the shift, VSVG did not colocalize with Golgi markers (unpublished data). 3 min after the shift (A), VSVG colocalized with GM130; 7 min after the shift, VSVG was located in one or two cisternae at the center of the stack (B) flanked by unlabeled cisternae, or colocalized with GT in trans cisternae (C) but not with GM130 (unpublished data). Note that the cis cisternae were not labeled. 11 min after the shift, VSVG colocalized with TGN46 (D). After 15 min, VSVG had left the stack (E). (F and G) Cells were fixed at 7 min and labeled by the immunoperoxidase technique. The ER accumulation–pulse protocol was used in the experiments in F and G. (G) Two serial sections of a stack containing two labeled central cisternae flanked by unlabeled elements. Bar: (A, D, and E) 130 nm, (B) 80 nm; (C, F, and G) 200 nm.

stricted to one (sometimes two) cisternae, located near the center of the stack (made up of four to five cisternae), with the adjacent proximal and distal cisternae completely devoid of label (Fig. 5 B). In some stacks, VSVG had already reached the trans-Golgi pole at this time, as indicated by its colocalization with GT, but the two to three cis-most cisterna were devoid of VSVG (Fig. 5 C). Thus, at least in numerous stacks, cargo does not seem to equilibrate throughout the stacked cisternae during transit. Other stacks (~30%) were completely empty of label, and the rest contained more than two labeled cisternae (three or four), or were labeled throughout (unpublished data). All of the these populations of stacks were present in the same cell. The possible origin of the above different VSVG labeling patterns is discussed below. Later, at 11 min, a fraction of the VSVG-containing cisternae had reached the TGN (as judged from colocalization with the TGN46) (Fig. 5 D), but some VSVG still resided in TGN46-negative and GT-positive cisternae, and at 15 min, the TGN was nearly depleted of cargo, presumably as a consequence of transport to the plasmalemma (Fig. 5 E). When this experiment was repeated using the immunoperoxidase technique (able to detect lower concentrations of antigen) (Mironov et al., 2000), the same overall time course and labeling pattern were observed. Fig. 5, F–G, shows examples of stacks fixed and labeled during intra-Golgi transit, at min 7. Again, only one or two cisternae appeared to be labeled at the center of the stack. In conclusion, using appropriate conditions, a significant fraction of the stacks can indeed be made to receive a sharp and limited (in time and intensity) input of VSVG. This pool of VSVG appears to progress in the cis to trans direction without equilibrating across the stack, and thus, presumably, without gradual physical transfer from cisterna to cisterna.

An additional use of these data was to assess the rate of progression of cargo through the stack by measuring the degree of colocalization of VSVG with Golgi markers. At 3 min, >70% of VSVG colocalized with GM130, at 7 min with GT, and at 11 with TGN46 (unpublished data), in agreement with the rate determined by immunofluorescence (Fig. 3). Also, the time course of transport of PC-I aggregates was followed by immuno-EM, and found to be indistinguishable from that of VSVG (Fig. 6). The only difference was that PC-I was present in the cisternae in its usual aggregated form, whereas VSVG was distributed homogeneously along the length of the cisterna (Fig. 1 D). Of note is that the membrane surrounding PC-I–containing distensions contained also the Golgi enzyme GT (Fig. 6 B). Finally, to examine whether the two cargoes precisely comigrate through the Golgi, double labeling for VSVG and PC-I was carried out 7 min after release of the temperature block. The cargoes colocalized closely, as illustrated in Fig. 6 D, in line with the immunofluorescence shown in Figs. 2 and 3. This colocalization was then quantified. This requires serial sections because VSVG prefers to localize on the flat portion of the cisterna than on PC-I distensions, and hence the two cargoes are often not found in the same section. Preembedded samples nanogold labeled for VSVG were serial sectioned. PC-I distensions and VSVG colocalized in ~80% of the cases (unpublished data). Presumably, the remaining 20% reflect arrival of the two cargoes in separate IC carriers.

The second question in this section is whether VSVG is excluded from Golgi vesicles during intra-Golgi traffic. Al-

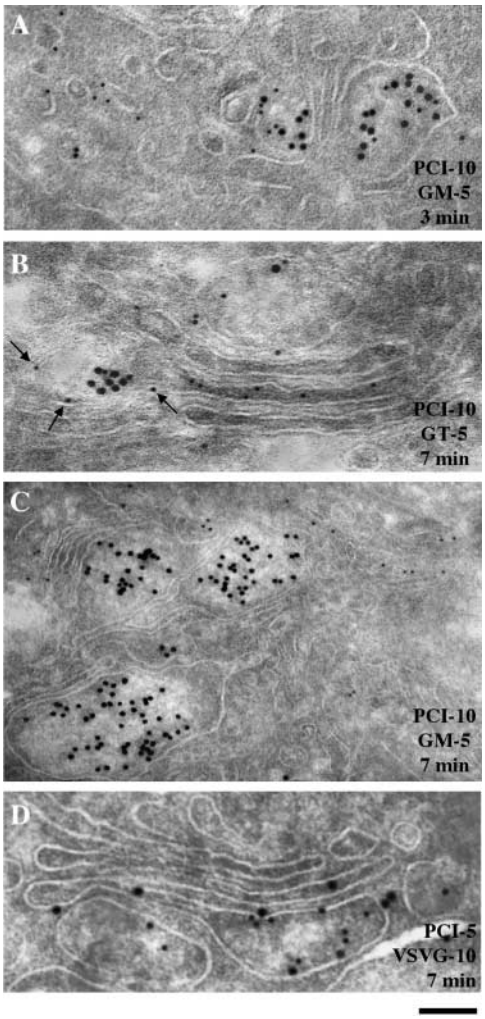

Figure 6. **Transit of PC-I aggregates through the Golgi stack.** Human fibroblasts were subjected to the small-pulse protocol, fixed at the times indicated below after release of the 15°C block, and prepared for immunogold labeling for PC-I (10-nm particles in A–C, 5-nm particles in D), VSVG (10-nm particles in D) and the Golgi markers GM130, GT, and TGN46 (5-nm particles). 3 min after the shift (A), VSVG colocalized with GM130; 7 min after the shift, VSVG colocalized with GT (B) but not with GM130 (C). Note that GT is present in the membrane surrounding the aggregate (arrows). (D) PC and VSVG colocalize at one pole of the stack. Bar: (A and B) 80 nm; (C) 130 nm; (D) 60 nm.

though VSVG has been found in COPI vesicles at concentrations comparable to those in cisternae (Orci et al., 1986, 1993) in in vitro Golgi preparations, to our knowledge, analogous data in living cells have not been reported thus far. For this analysis we used not only the small-pulse (Fig. 5), but also the large-pulse and the ER accumulation–chase protocols, which generate higher fluxes of membrane and cargo through the Golgi. Cells (both fibroblasts and COS-7 cells) were fixed 8–9 min after release of the temperature block, i.e., when the flux through the stack is high. The analysis was limited to the vesicular profiles adjacent (lateral) to labeled cisternae (see Materials and methods). We assume that these profiles represent bona fide vesicles based on published evidence, including EM tomography data by Marsh et al. (2001) indicating that vesicles represent a major fraction of the round profiles in the vicinity of cisternae, and data of Orci et al. (1997), showing that most of these profiles are COPI coated. These vesicles can in principle derive from Golgi cisternae or from neighboring IC elements. To distinguish their origin, we labeled them for the IC marker GM130 (Marra et al., 2001). None of the vesicles was labeled, ruling out the IC as their source and indicating that they derive from the Golgi stack. Cells were then labeled for VSVG to determine its level in the Golgi vesicles. Several labeling methods were used to avoid systematic artifacts. First, we used the cryoimmunogold technique and an antibody against a lumenal VSVG epitope. The Golgi stacks were abundantly labeled, whereas only a few gold particles were found in the neighboring vesicular profiles (Fig. 7, A and B). Morphometry showed that the density of particles was sixfold lower in vesicular profiles than in adjacent cisternae (Table I). The density ratio between the two structures was not affected by the level of expression of VSVG, which varied up to threefold between different cells (unpublished data). To rule out the possibility that the lumenal VSVG antigen in vesicles might be masked by lumenal proteins or might be less accessible than in cisternae because of geometry factors, we next used an antibody against a cytosolic VSVG epitope. The ratio between cisternal and vesicular labeling densities remained close to six (unpublished data). The same experiment (using the cytosolic epitope) was then repeated using the preembedding nanogold gold enhance technique, in which the problems of epitope accessibility are different than those encountered in cryogold labeling. Under these conditions, the ratio was close to eight (Fig. 7 C; Table I). The preembedding immunoperoxidase technique using an antibody against the lumenal VSVG epitope was also applied. The results in panel 7 D (tangential semithick section of a cisterna) again show intense labeling in cisternae but no labeling in vesicular profiles. Finally, we used another antigen and a radically different approach. Cells were transfected with secretory soluble HRP (ssHRP) (Connolly et al., 1994), whose detection is free of all the problems related to the access of antibody to epitope, and fixed at steady state (ssHRP cannot be synchronized). Cells were fixed and subjected to the HRP reaction procedure. Once again, vesicular profiles were depleted of cargo, i.e., unstained, whereas most of the cisternae were stained, often intensely (Fig. 7, E and F), indicating that secretory HRP is much less concentrated in vesicles than in cisternae. In summary, by using a variety of labeling techniques, we find that small diffusible secretory proteins are depleted in Golgi vesicles as compared with the stack.

Table I. **Distribution of VSVG within Golgi membranous structures**

	Cisternae	Round (>65 nm) vesicular profiles	Buds
Nanogold	1.34 ± 0.12	0.16 ± 0.02	0.2 ± 0.05
Cryogold	3.8 ± 0.4	0.64 ± 0.05	ND

Linear density of gold labeling for VSVG expressed as the number of gold particles per intersection between the profiles attributed to each structure (cisternae, vesicles, buds) with the lines of the test grid. Values represent mean ± SEM obtained by analyzing 40 (nanogold) and 20 Golgi stacks (cryogold). Background labeling was low, between 0.01 and 0.015 for both methods.

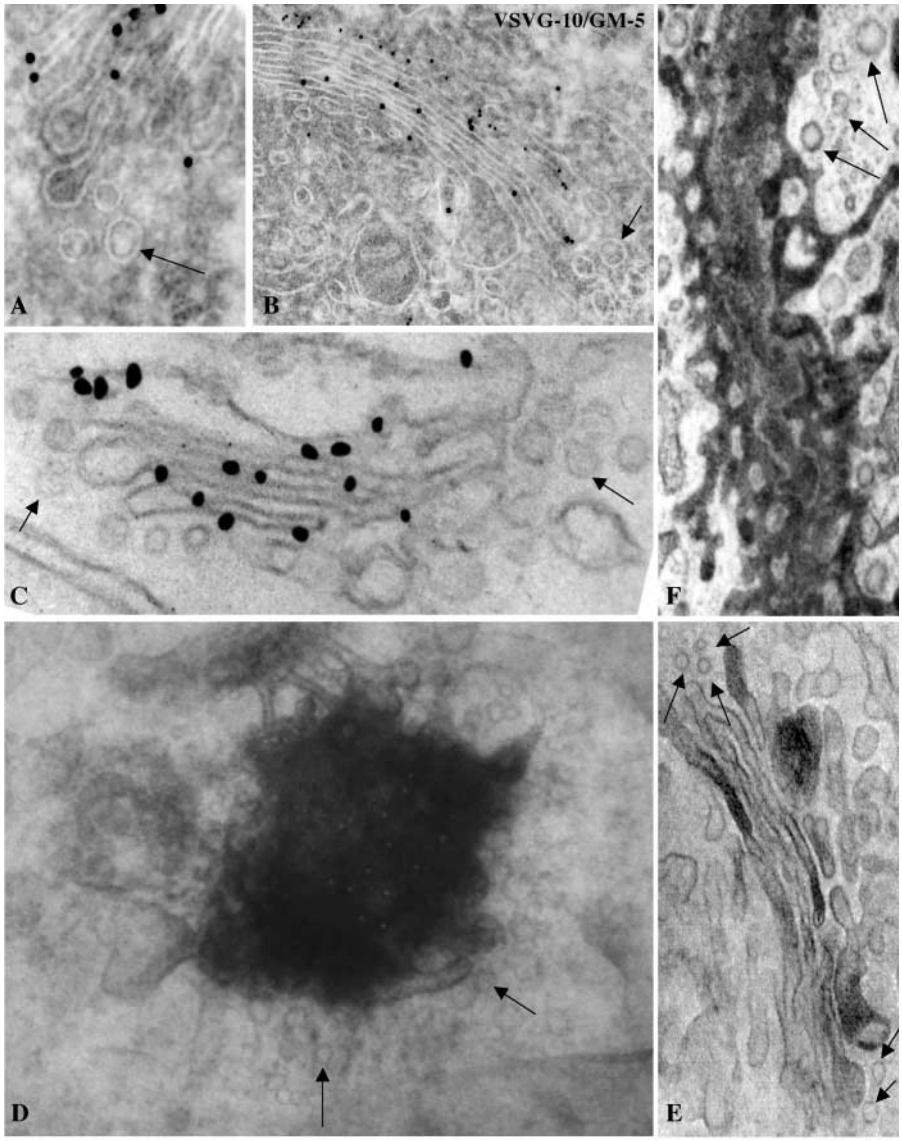

Figure 7. **VSVG and ssHRP are excluded from Golgi vesicles during transit through the Golgi complex.** Human fibroblasts (A–C) and COS-7 cells (D–F) were subjected to the ER accumulation–chase protocol (D) or the large (C) or the intermediate (A and B) pulse protocols, fixed 7 min after the release of the temperature block (A–D), and then processed for labeling. In the experiments in (A) and (B) they were labeled for VSVG by the cryo-immunogold technique, in C by the nanogold gold enhance technique, and in D (which shows a tangential thick section), by the preembedding immunoperoxidase method. Also in A, the GM130 protein is labeled (small particles). (E and F) For ssHRP experiments, COS-7 cells were transfected with ssHRP, fixed at steady state, and then processed for detection of HRP. (E) Perpendicular and (F) tangential section. Irrespective of the labeling and sectioning technique, the round (vesicular) profiles (arrows) are almost always devoid of cargo, whereas cisternae are labeled. Bar: (A, D, and E) 110 nm; (B) 120 nm; (C) 90 nm; (F) 200 nm.

As noted above, not all stacks in the same cell are labeled in one to two cisternae during intra-Golgi traffic. Some are empty and some contain cargo in more than two cisternae. The simplest interpretation of this heterogeneity is that different stacks receive different numbers of labeled IC elements, for different lengths of time. Stacks containing only one or two labeled cisterna may have received very few and simultaneous inputs from the IC, those labeled in many cisternae have incorporated several IC elements over a few minutes, and the empty stacks have received no cargo. A corollary of this is that, under the small-pulse conditions, the stacks should not exchange VSVG freely along the ribbon, otherwise they would present similar labeling patterns. Because this possibility is relevant in discriminating between traffic mechanisms (see Discussion), we sought to verify it in GFP-based experiments in living cells. Both human fibroblasts and COS-7 cells were transfected with VSVG–GFP, subjected to the small-pulse protocol, and examined from minutes 6 to 12 after releasing the temperature block (i.e., while VSVG is traversing the stack). VSVG–GFP was localized in 10–30 discrete elongated spots of variable intensity and with an apparent length of 1–2 microns (Fig. 8, A–E). If cells are fixed and stained for a Golgi marker, it appears that the spots fill only part of the ribbon (Fig. 8, H–M). These spots are identical to those shown before in Figs. 2 and 3. Correlative video light EM shows that these spots represent VSVG–GFP within cisternae of individual stacks (Fig. 8, F–G). To examine whether the VSVG-carrying stacks could exchange VSVG, we photobleached half of the Golgi area and examined the recovery of fluorescence (Lippincott-Schwartz et al., 2000). No recovery was observed (Fig. 8, D–E; Video 1, available at http://www.jcb.org/cgi/content/full/jcb.200108073/DC1). Thus, these results are in line with the EM data and confirm that, under the small-pulse protocol, stacks do not exchange VSVG, at least over the time scale of intra-Golgi traffic. Importantly, the restricted mobility of VSVG was not due to the fact that the stacks are physically isolated from each other, because analogous experiments with GT-GFP showed that this enzyme have a normal ribbon-like distribution and recovers fluorescence after photobleaching (unpublished data). An implication of these data is that VSVG partitions between connected Golgi

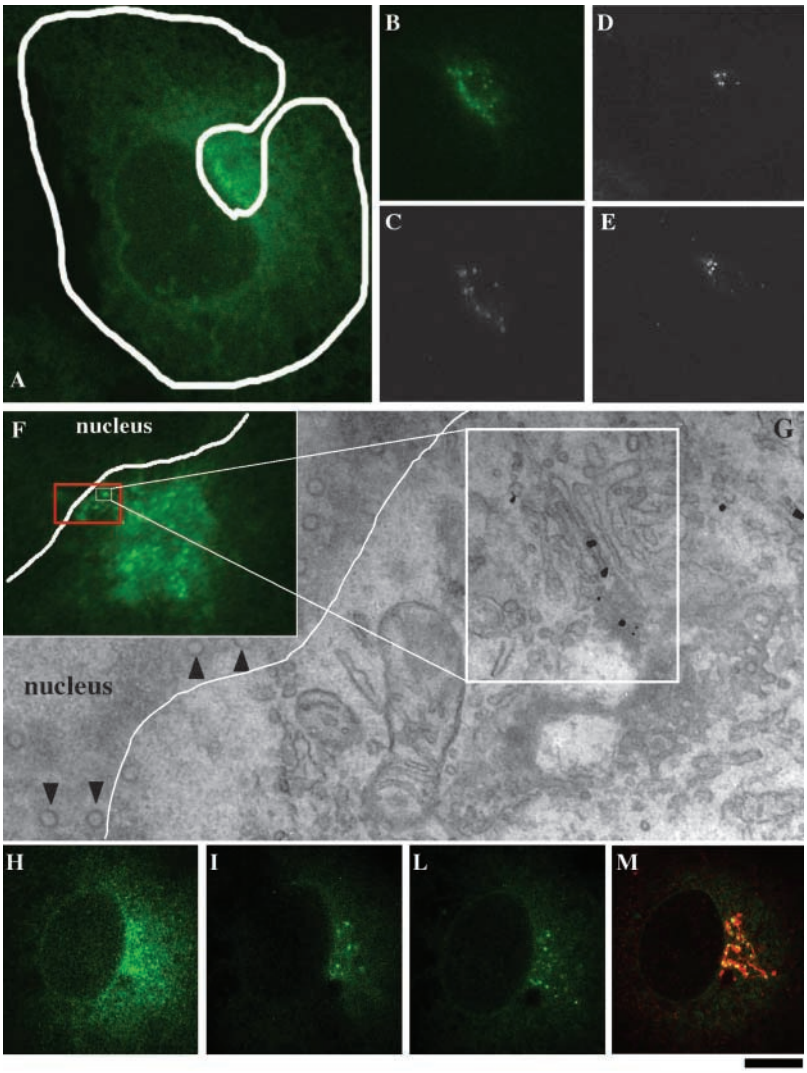

Figure 8. **Dynamic behavior of VSVG-GFP during intra-Golgi transport.** Cell were transfected with VSVG–GFP, placed on glass bottom microwell dishes with coordinated grids, subjected to the small-pulse protocol, and studied, after releasing the 15°C block, by laser scanning confocal microscope and time-lapse analysis. (A) 4 min after the shift, the Golgi spots containing VSVG–GFP in the central Golgi area were masked by the high ER background. (B and C) Repeated bleaching of the whole cell (except the Golgi area, delineated) removed the ER background and made the spotty pattern of the VSVG in the Golgi zone more evident. (D and E) Half of the Golgi area was bleached and observed 1 min (D) and 5 min (E) after bleaching. No fluorescence recovery was observed. (Video 1, available at http://www.jcb.org/cgi/content/full/jcb.200108073/DC1). (F and G) This cell was fixed 7 min after releasing the 15°C block and prepared for correlative video light EM using the nanogold gold enhancement method. The region at the center of the white square in (F) was analyzed (it corresponds to the square is the area enlarged in G). As can be seen in G, the spot represents a stack containing VSVG–GFP in a central cisterna (large white square) Arrowheads indicate nuclear pores. (H–M) Cells were treated as for the experiment in panels B and C and observed at 4 min; (H) Image before bleaching; (I) 7 min; (L) 11 min after releasing the temperature block. At 11 min (when some of the spots were starting to leave the Golgi area) it was fixed an stained for TGN46 (red) and VSVG (green) (M). Many of the spots colocalize with the ribbon, whereas others are probably moving out. Bar: (A–E and H–M) 15 μm; (F) 8 μm; (G) 300 nm.

domains. We are not aware of published observations of this type, possibly because previous investigators have generally used large cargo load protocols that induce a diffuse cargo distribution overlapping with that of Golgi markers. A full analysis of these results would be beyond the scope of this paper and will be pursued separately.

Discussion

Kinetic and mechanistic evidence for a single transport mechanism for PC-I and VSVG

The kinetic argument for a single mode of transport is based on the notion that the rate of traffic, although influenced by numerous variables, is a function of the underlying mechanism (Mironov et al., 1998; Pelham and Rothman, 2000). Hence, the fact that PC-I and VSVG transit through the Golgi together under different conditions, indicates that the two cargoes move by a single process. The mechanistic evidence supports the same conclusion: neither VSVG nor PC-I need to leave the lumen of cisternae via vesicular carriers to transit through the Golgi, confirming that the two proteins use the same mode of traffic.

With regard to PC-I, this point was established by 3-D reconstructions of Golgi PC-I aggregates, showing that they always reside within the cisternal lumen. As noted before, these findings differ from those of Volchuk at al. (2000), who observed the presence of the large artificial FK506-binding protein (FKBP)-containing secretory aggregates in megavesicles flanking the stack during cargo progression. This difference can be explained in at least two ways. On the one hand, there is no conceptual obstacle to thinking that different cargoes might use different secretory mechanisms (Mironov et al., 1997); FKBP-containing aggregates might enter large vesicles whereas others (PC-I) may not, for reasons still to be understood. On the other hand, it should be considered that the presence of FKBP-containing megavesicles in the vicinity of Golgi stacks does not represent proof that these structures function as intra-Golgi transport intermediates. Given the experimental design by which megavesicles were observed, which involves a block at 15°C, and therefore the accumulation of aggregates in the IC, a possible explanation for the appearance of these structures near the cisternae is that they might be aggregate-containing IC elements approaching the edge of the Golgi stack after release of the temperature block (in keeping with our observation that IC membranes often reach the stack from its side). PC-I cannot give rise to IC-derived megavesicles because it

reaches the Golgi as separate trimers, and coalesces into visible aggregates only after entering the lumen of the cis cisterna (Cho and Garant, 1981; Leblond, 1989).

Regarding VSVG, the conclusion that it moves, like PC-I, through the Golgi without a need for anterograde dissociative carriers, rests on two complementary lines of evidence. First, at least under small-pulse conditions, VSVG can be shown to traverse the stack while remaining confined within only one or two cisternae. The simplest interpretation of this is that transport can occur without involving gradual physical transfer of VSVG from cisterna to cisterna, otherwise it would be accompanied by the formation of a VSVG gradient across the stack (an alternative theoretical possibility may be that all of the VSVG molecules in one cisterna would simultaneously transfer into the next, but this mechanism appears far fetched at present). Second, Golgi vesicles were markedly depleted of VSVG (six- to eightfold), in agreement with the findings of Martínez-Menárguez et al. (2001), who report an even more dramatic depletion of VSVG in Golgi vesicles. Such a degree of exclusion is difficult to reconcile with a role of vesicles as VSVG carriers (although, again, not theoretically incompatible with such a role; for instance, extremely fast shuttling of partially depleted vesicles might suffice to support VSVG intra-Golgi transport). Thus, when taken separately, each of the above two lines of evidence represent strong but not conclusive proof against Golgi vesicles as carriers; combined, they make the possibility of a major role of such vesicles in anterograde transport of VSVG extremely unlikely.

VSVG is not the only reported example of cargo exclusion from Golgi vesicles in living cells. Albumin and apolipoprotein E are depleted in Golgi vesicles in hepatocytes (Dahan et al., 1994), the ssHRP chimera is excluded in COS-7 Golgi vesicles (this paper) and scales (even scales so small in size that they could easily fit into vesicles) are excluded from vesicles in the algal cell Scherfelia dubia (Becker et al., 1995). An exception appears to be proinsulin, which is present in vivo in vesicles at concentrations comparable to those in cisternae (Orci et al., 1997). Thus, it is possible that a class of secretory proteins might be transported via Golgi vesicles.

Nature of the transport mechanism

What is then the transport mechanism for VSVG and PC-I? Clearly, as discussed above, our results are inconsistent with the anterograde vesicular traffic model. They are also hard to reconcile with the traffic-via-continuities scheme in its simplest form, which envisions a key role for cargo flow across adjacent stacks in the ribbon (Mironov et al., 1997, 1998). This is based on two considerations: first, it is difficult to imagine large PC-I aggregates flowing along the Golgi at the same rate as VSVG, and, second, at least under the small-pulse protocol, VSVG can traverse the Golgi without diffusing along the Golgi ribbon (Fig. 8). Notably, the latter data do not exclude the possibility of diffusion of VSVG within the Golgi (indeed, this has been observed by Storrie et al., in 1994 and by ourselves, using large load protocols; unpublished data); however, they do tend to rule out long range cargo diffusion along the ribbon as a fundamental feature of intra-Golgi transport.

In contrast, the cisternal maturation model is compatible with most of the available evidence so far both in vivo (Introduction; Wooding and Pelham, 1998; Morin-Ganet et al., 2000), and in vitro (Love et al., 1998; Lanoix et al., 1999). Nevertheless, it is important to note that although a central feature of this model (i.e., progression of cargo without dissociation from cisternae) has been verified in our experiments, many of its elements as popularized in several reviews remain hypothetical. For instance, we do not know (if indeed the classical maturation scheme applies) how the retrograde traffic of enzymes is regulated, or how incoming IC membranes would be added to the stack at the cis pole and, finally, how membranes may be removed from the trans side at corresponding rates.

Thus, other traffic models cannot be excluded at this time. For example, intra-Golgi traffic could begin with the fusion of GM130-positive cargo-containing IC elements with the cis cisterna, forming a new mixed compartment from which, later, the GM130-positive membrane would be segregated and retrieved back into the IC (Marra et al., 2001); the same sequence of events (fusion, mixing, and resegregation) could occur again at each transfer step. Of note, this scheme has features of the maturation model, and includes a role for transient short range membrane continuities (Mellman and Simons, 1992; Mironov et al., 1997, 1998).

In conclusion, this report, by showing that both small diffusible and large supramolecular cargoes can traverse the Golgi without leaving the lumen of cisternae, puts new constraints on our way of thinking about biosynthetic traffic. More work using the sort of concepts and approaches applied here will hopefully help further elucidate the organization of the secretory pathway.

Materials and methods

Cells, treatments, DNA constructs, antibodies, and reagents

Human skin fibroblasts, a gift from Dr. M. De Luca (Instituto Dermopatico Dell'Immacolata, Rome, Italy), were cultured in DME with 10% calf serum, and stimulation of PC-I synthesis was achieved by incubating in DME containing 1% adult calf serum without AA for at least 3 h. Transfections were carried out by electroporation (1 μg cDNA per 2×10^5 cells, V = 380 v, C = 850 μF) and infections with ts045-VSV, as previously described (Polishchuk et al., 2000). For traffic synchronization, cells were infected with ts045-VSV at 32°C or transfected with VSVG–GFP or ssHRP, a gift from Dr. D. Cutler (Medical Research Center, London, UK), by electroporation and held at 40°C for 12 h, shifted to 32°C, and then treated as described in Fig. 1 and text.

The following antibodies were used: rabbit polyclonal antibodies against GM130, a gift from Dr. M.A. De Matteis (Mario Negri Sud Institute, Chieti, Italy); the COOH-terminal peptide of the α-1 chain of PC-I, a gift from Dr. L.W. Fisher (National Institutes of Health, Bethesda, MD); GT, and the lumenal domain of VSVG, a gift from Dr. K. Simons (Max Planck Institute, Dresden, Germany); a sheep polyclonal antibody against TGN46, a gift from Dr. S. Ponnambalam (Leeds University, Leeds, UK); and monoclonal antibodies against the helical portion of PC-I (Fuij Chemical Industries), the lumenal domain of VSVG (17.2.21.4), a gift from Dr. J. Gruenberg (University of Geneva, Geneva, Switzerland), giantin, a gift from Dr. H.-P. Hauri (University of Basel, Basel, Switzerland), and the cytosolic tail of VSVG (P5D4) (Sigma-Aldrich). Nanogold-conjugated Fab fragments of anti–rabbit IgG and Gold Enhancer were from Nanoprobes (Yaphank). Protein A conjugated with colloidal gold was from Dr. J. Slot (Utrecht University, Utrecht, Netherlands). Anti–rabbit, anti–mouse, and anti–sheep antibodies conjugated with Alexa 488, Alexa 546, and Alexa 633 were from Molecular Probes. Unless otherwise noted, all other chemicals and reagents were obtained from previous sources (Bonfanti et al., 1998; Polishchuk et al., 2000) or from Sigma-Aldrich.

Immunofluorescence, measurement of the degree of colocalization of immunofluorescent proteins, and GFP-based time-lapse analysis

Immunofluorescence experiments and GFP-based time-lapse analysis were performed by laser scanning confocal microscopy as described (Polishchuk et al., 2000). To quantify the degree of colocalization between VSVG and the Golgi markers in Fig. 3, a pair of proteins was labeled in each experiment. Cargo proteins (VSVG and PC-I) and Golgi markers (GM130, GT, and TGN46) (Fig. 3) were labeled with CY3 (red) and Alexa 488 (green), respectively. Optical sections passing through the area with the highest labeling intensity for cargo proteins were acquired using an LSM 510 laser scanning confocal microscope (Zeiss), without subtraction of background and with a pinhole size optimized to have all intensity values between 1 and 254 (linear range). Sampling of cells was performed randomly, and only the Golgi area was used. To quantify the level of colocalization, the scatter diagram function of the LSM software was used. Only the spots labeled for cargo (Fig. 3) were considered. In each cargo-containing pixel, the intensity of the appropriate Golgi marker was measured. Colocalization was considered positive if the intensity of the Golgi marker fluorescence was not more than twofold higher or twofold lower than the intensity of the cargo fluorescence in the same pixel. Because fluorescence intensities depend on labeling conditions, in each experiment conditions were calibrated to give a VSVG/marker ratio close to one (1) in the spots where colocalization was obviously occurring. All samples were processed equally and evaluated in a blind fashion. Similar levels of laser power (~25%) and detector amplification were used for both channels. The percentage of colocalization-positive pixels was then estimated.

Conventional and correlative EM, immuno-EM, and morphometry

Conventional (Epoxy-embedding) EM (Bonfanti et al., 1998), correlative video light EM (Polishchuk and Mironov, 2001), correlative light EM and nanogold enhancement (Marra et al., 2001), and ultrathin cryosectioning (Peters, 2001) were carried out as previously described. In morphometry experiments, round profiles adjacent (lateral) to labeled cisternae not labeled for GM130 (a marker of the CGN and late IC) (Marra et al., 2001), and not exceeding 65 nm in diameter, a feature of COPI-dependent vesicles (Marsh et al., 2001), were considered as COPI-derived vesicles. It has been shown by Marsh et al. (2001) that small 52-nm vesicles form the vast majority of round profiles on random ultrathin sections. The labeling density of tsVSVG in cisternae and surrounding round profiles was estimated according to Lucocq (1993) and expressed as the number of gold particles per intersection. Colocalization between cargoes (10-nm particles) and Golgi markers (GM130, GT, and TGN, 5-nm particles) was considered positive if the 5- and 10-nm gold particles were localized within the same membrane structure.

Rapid freezing cryosubstitution, serial sectioning, 3-D reconstruction, and electron tomography

Cells were rapidly frozen as described by Heuser et al. (1979) and cryosubstituted as described by Nicolas et al. (1989). Thin serial sectioning and 3-D reconstructions were performed as previously described (Bonfanti et al., 1998). The analysis of samples by electron tomography was performed as previously described (Koster et al., 1997; Ladinsky et al., 1999). In brief, thick (250 nm) sections of chemically fixed samples were covered with 10 nm colloidal gold. Next, automated data acquisition was carried out as described (Ziese et al., 2001) on a Tecnai 20 electron microscope at 200 kV (FEI/Philips Electron Optics) equipped with a slow-scan CCD camera (TemCam F-214; TVIPS GmbH) and a computerized goniometer. Finally, after alignment of the data stack using the colloidal gold as fiducial markers and reconstruction with the IMOD program package (Kremer et al., 1996), 2–3-nm virtual slices were extracted from the tomograms and visualized. Object surfaces were rendered using the SURFdriver and IMOD softwares.

Online supplemental material

Video 1, available at http://www.jcb.org/cgi/content/full/jcb.200108073/DC1, shows VSVG–GFP in the Golgi complex (FRAP). COS 7 cells were transfected with VSVG–GFP, placed on glass-bottom microwell dishes with coordinated grids, subjected to small-pulse protocol, and examined by laser scanning confocal microscope. 4 min after the shift from 15°C to 40°C, the Golgi spots containing VSVG–GFP in the central Golgi area were masked by a high-ER background. To remove this background, the whole cell, except the Golgi area, was repeatedly bleached. This made the fluorescent spots in the Golgi zone more evident. These spots hovered within the Golgi area without exhibiting long-range movements. Next, at 6–7 min, half of the Golgi area was bleached to examine whether fluorescence would recover in the bleached spots. No recovery was observed. 10 min after the shift from 15°C to 40°C, the GFP-containing spots became more mobile and began to leave the Golgi area.

We thank Dr. R. Le Donne and A. Cavallo for excellent secretarial assistance and artwork preparation, Drs. M. De Luca, M.A. De Matteis, L.W. Fisher, K. Simons, S. Ponnambalam, J. Gruenberg, H.-P. Hauri, and D. Cutler for providing us with cell lines, antibodies, and cDNA constructs, and C. P. Berrie for critically reading of the manuscript.

We acknowledge financial support from the Italian Association for Cancer Research, Telethon (grants E.0982, E.1105, and E.1249), the Italian National Research Council (contract 99.00133.PF49), INTAS (project 991-1732), and the postdoctoral fellowship program from Korea Science and Engineering Foundation (to H.-S. Kweon). A.J. Koster is supported by the Royal Netherlands Academy of Arts and Sciences (KNAW), and W.J.C. Geerts and K.N.J. Burger are supported by FEI/Philips Electron Optics.

Submitted: 15 August 2001
Revised: 12 November 2001
Accepted: 12 November 2001

References

Bannykh, S.I., and W.E. Balch. 1997. Membrane dynamics at the endoplasmic reticulum-Golgi interface. *J. Cell Biol.* 138:1–4.

Becker, B., B. Bolinger, and M. Melkonian. 1995. Anterograde transport of algal scales through the Golgi complex is not mediated by vesicles. *Trends Cell Biol.* 5:305–307.

Bergmann, J.E. 1989. Using temperature-sensitive mutants of VSV to study membrane protein biogenesis. *Methods Cell Biol.* 32:85–110.

Bonfanti, L., A.A. Mironov, Jr., J.A. Martinez-Menarguez, O. Martella, A. Fusella, M. Baldassarre, R. Buccione, H.J. Geuze, A.A. Mironov, and A. Luini. 1998. Procollagen traverses the Golgi stack without leaving the lumen of cisternae: evidence for cisternal maturation. *Cell.* 95:993–1003.

Bruckner, P., and E.E. Eikenberry. 1984. Procollagen is more stable in cellulo than in vitro. *Eur. J. Biochem.* 140:397–399.

Cho, M.I., and P.R. Garant. 1981. An electron microscopic radioautographic study of collagen secretion in periodontal ligament fibroblasts of the mouse: I. Normal fibroblasts. *Anat. Rec.* 201:577–586.

Connolly, C.N., C.E. Futter, A. Gibson, C.R. Hopkins, and D.F. Cutler. 1994. Transport into and out of the Golgi complex studied by transfecting cells with cDNAs encoding horseradish peroxidase. *J. Cell Biol.* 127:641–652.

Dahan, S., J.P. Ahluwalia, L. Wong, B.I. Posner, and J.J. Bergeron. 1994. Concentration of intracellular hepatic apolipoprotein E in Golgi apparatus saccular distensions and endosomes. *J. Cell Biol.* 127:1859–1869.

Erk, I., G. Nicolas, A. Caroff, and J. Lepault. 1998. Electron microscopy of frozen biological objects: a study using cryosectioning and cryosubstitution. *J. Microsc.* 189:236–248.

Glick, B.S., and V. Malhotra. 1998. The curious status of the Golgi apparatus. *Cell.* 95:883–889.

Griffiths, G. 2000. Gut thoughts on the Golgi complex. *Traffic.* 1:738–745.

Harwood, R., M.E. Grant, and D.S. Jackson. 1976. The route of secretion of procollagen. The influence of alphaalpha′-bipyridyl, colchicine and antimycin A on the secretory process in embryonic-chick tendon and cartilage cells. *Biochem. J.* 156:81–90.

Heuser, J.E., T.S. Reese, M.J. Dennis, Y. Jan, L. Jan, and L. Evans. 1979. Synaptic vesicle exocytosis captured by quick freezing and correlated with quantal transmitter release. *J. Cell Biol.* 81:275–300.

Koster, A.J., R. Grimm, D. Typke, R. Hegerl, A. Stoschek, J. Walz, and W. Baumeister. 1997. Perspectives of molecular and cellular electron tomography. *J. Struct. Biol.* 120:276–308.

Kremer, J.R., D.N. Mastronarde, and J.R. McIntosh. 1996. Computer visualization of three-dimensional image data using IMOD. *J. Struct. Biol.* 116:71–76.

Kuismanen, E., and J. Saraste. 1989. Low temperature-induced transport blocks as tools to manipulate membrane traffic. *Methods Cell Biol.* 32:257–274.

Ladinsky, M.S., D.N. Mastronarde, J.R. McIntosh, K.E. Howell, and L.A. Staehelin. 1999. Golgi structure in three dimensions: functional insights from the normal rat kidney cell. *J. Cell Biol.* 144:1135–1149.

Lanoix, J., J. Ouwendijk, C.C. Lin, H. Stark, H.D. Love, J. Ostermann, and R. Nilsson. 1999. GTP hydrolysis by arf-1 mediates sorting and concentration

of Golgi resident enzymes into functional COP I vesicles. *EMBO J.* 18: 4935–4948.

Leblond, C.P. 1989. Synthesis and secretion of collagen by cells of connective tissue, bone, and dentin. *Anat Rec.* 224:123–138.

Lippincott-Schwartz, J., T.H. Roberts, and K. Hirschberg. 2000. Secretory protein trafficking and organelle dynamics in living cells. *Annu. Rev. Cell Dev. Biol.* 16:557–589.

Love, H.D., C.C. Lin, C.S. Short, and J. Ostermann. 1998. Isolation of functional Golgi-derived vesicles with a possible role in retrograde transport. *J. Cell Biol.* 140:541–551.

Lucocq, J. 1993. Particulate markers for immunoelectron microscopy. *In* Fine Structure Immuno-cytochemistry. Vol. Chapter 8. G. Griffiths, editor. Springer-Verlag, Germany. 279–302.

Lyles, D.S., and M.O. McKenzie. 1998. Reversible and irreversible steps in assembly and disassembly of vesicular stomatitis virus: equilibria and kinetics of dissociation of nucleocapsid-M protein complexes assembled in vivo. *Biochemistry.* 37:439–450.

Malhotra, V., L. Orci, B.S. Glick, M.R. Block, and J.E. Rothman. 1988. Role of an N-ethylmaleimide-sensitive transport component in promoting fusion of transport vesicles with cisternae of the Golgi stack. *Cell.* 54:221–227.

Marra, P., T. Maffucci, T. Daniele, G. Di Tullio, Y. Ikehara, E.K.L. Chan, A. Luini, G. Beznoussenko, A. Mironov, and M.A. De Matteis. 2001. The Golgi matrix proteins GM130 and GRASP65 cycle through a novel subdomain of the intermediate compartment. *Nat. Cell Biol.* 3:1101–1113.

Marsh, B.J., D.N. Mastronarde, K.F. Buttle, K.E. Howell, and J.R. McIntosh. 2001. Organellar relationships in the Golgi region of the pancreatic beta cell line, HIT-T15, visualized by high resolution electron tomography. *Proc. Natl. Acad. Sci. USA.* 98:2399–2406.

Martínez-Menárguez, J.A., R. Prekeris, V.M.J. Oorschot, R. Scheller, J.W. Slot, H.J. Geuze, and J. Klumperman. 2001. Peri-Golgi vesicles contain retrograde but not anterograde proteins consistent with the cisternal-progression model of intra-golgi transport. *J. Cell Biol.* 155:1213–1224.

Mellman, I., and K. Simons. 1992. The Golgi complex: in vitro veritas? *Cell.* 68: 829–840.

Mellman, I., and G. Warren. 2000. The road taken: past and future foundations of membrane traffic. *Cell.* 100:99–112.

Mironov, A.A., P. Weidman, and A. Luini. 1997. Variations on the intracellular transport theme: maturing cisternae and trafficking tubules. *J. Cell Biol.* 138: 481–484.

Mironov, A., Jr., A. Luini, and A. Mironov. 1998. A synthetic model of intra-Golgi traffic. *FASEB J.* 12:249–252.

Mironov, A.A., R.S. Polishchuk, and A. Luini. 2000. Visualizing membrane traffic in vivo by combined video fluorescence and 3-D electron microscopy. *Trends Cell Biol.* 10:349–353.

Morin-Ganet, M.N., A. Rambourg, S.B. Deitz, A. Franzusoff, and F. Kepes. 2000. Morphogenesis and dynamics of the yeast Golgi apparatus. *Traffic.* 1:56–68.

Nicolas, M.T., J.M. Bassot, and G. Nicolas. 1989. Immunogold labeling of luciferase in the luminous bacterium Vibrio harveyi after fast-freeze fixation and different freeze-substitution and embedding procedures. *J. Histochem. Cytochem.* 37:663–674.

Orci, L., B.S. Glick, and J.E. Rothman. 1986. A new type of coated vesicular carrier that appears not to contain clathrin: its possible role in protein transport within the Golgi stack. *Cell.* 46:171–184.

Orci, L., D.J. Palmer, M. Ravazzola, A. Perrelet, M. Amherdt, and J.E. Rothman. 1993. Budding from Golgi membranes requires the coatomer complex of non-clathrin coat proteins. *Nature.* 362:648–652.

Orci, L., M. Stamnes, M. Ravazzola, M. Amherdt, A. Perrelet, T.H. Sollner, and J.E. Rothman. 1997. Bidirectional transport by distinct populations of COPI-coated vesicles. *Cell.* 90:335–349.

Pelham, H.R., and J.E. Rothman. 2000. The debate about transport in the Golgi: two sides of the same coin? *Cell.* 102:713–719.

Peters, P. 2001. Cryoimmunogold electron microscopy. *In* Current Protocols in Cell Biology. J.S. Bonifacino, M. Dasso, J.B. Harford, J. Lippincott-Schwartz, and K.M. Yamada, editors. John Wiley & Sons, New York. 4.8.1–4.8.9.

Polishchuk, R.S., and Mironov, A.A. 2001. Correlative video/light electron microscopy. *In* Current Protocols in Cell Biology. J.S. Bonifacino, M. Dasso, J.B. Harford, J. Lippincott-Schwartz, and K.M. Yamada, editors. John Wiley & Sons. New York. 4.8.1–4.8.9.

Polishchuk, R.S., E.V. Polishchuk, P. Marra, S. Alberti, R. Buccione, A. Luini, and A.A. Mironov. 2000. Correlative light-electron microscopy reveals the tubular-saccular ultrastructure of carriers operating between Golgi apparatus and plasma membrane. *J. Cell Biol.* 148:45–58.

Rothman, J.E., and F.T. Wieland. 1996. Protein sorting by transport vesicles. *Science.* 272:227–234.

Schekman, R., and L. Orci. 1996. Coat proteins and vesicle budding. *Science.* 271: 1526–1533.

Storrie, B., R. Pepperkok, E.H. Stelzer, and T.E. Kreis. 1994. The intracellular mobility of a viral membrane glycoprotein measured by confocal microscope fluorescence recovery after photobleaching. *J. Cell Sci.* 107:1309–1319.

Volchuk, A., M. Amherdt, M. Ravazzola, B. Brugger, V.M. Rivera, T. Clackson, A. Perrelet, T.H. Sollner, J.E. Rothman, and L. Orci. 2000. Megavesicles implicated in the rapid transport of intracisternal aggregates across the Golgi stack. *Cell.* 102:33–48.

Weidman, P.J. 1995. Anterograde transport through the Golgi complex: do Golgi tubules hold the key? *Trends Cell Biol.* 5:302–305.

Wooding, S., and H.R. Pelham. 1998. The dynamics of Golgi protein traffic visualized in living yeast cells. *Mol. Biol. Cell.* 9:2667–2680.

Ziese, U., A.H. Janssen, J.L. Murk, W.J.C. Geerts, T. van der Krift, A.J. Verkleij, and A.J. Koster. 2001. Automated high-throughput electron tomography by pre-calibration of image shifts. *J. Microscopy*. In press.